DOI: 10.1002/ejic.200500855

Comparative Sol–Hydro(Solvo)thermal Synthesis of TiO_2 Nanocrystals

Xianfeng Yang,[a] Hiromi Konishi,[b] Huifang Xu,[c] and Mingmei Wu*[a]

Keywords: Crystal growth / Nanostructures / Self-assembly / Solvothermal synthesis / Titanium

Three small inorganic compounds [acetic acid (CH_3COOH), nitric acid (HNO_3), and hydrochloric acid (HCl)] and five small organic compounds [*n*-butyl alcohol ($CH_3CH_2CH_2CH_2OH$), 1,2-propanediol ($CH_2OHCHOHCH_3$), propane-1,3-dicarboxylic acid ($HOOCCH_2COOH$), butane-1,4-dicarboxylic acid ($HOOCCH_2CH_2COOH$), and ethylenediamine ($H_2NCH_2CH_2NH_2$)] with different donors (Cl^-, NO_3^-, OH, COO^-, and NH_2) are used respectively and comparatively in different reaction media for tailoring the sol–hydrothermal synthesis of TiO_2 nanocrystals at a specific reaction temperature and/or for different reaction times. Both anatase and rutile with a variety of nanostructures such as nanocubes, nanorods, nanoneedles, and their self-assembled nanospheres are selectively grown. Well-defined and crystalline anatase nanocrystals with a narrow size distribution are prepared in the presence of *n*-butyl alcohol. With the use of HCl, nanoneedles and their assembled nanospheres of phase-pure rutile are obtained under much less drastic conditions, even at 100 °C and for only two hours. The effects of the reaction media, synthesis temperatures, and aging times on the structures and shapes of the products are investigated in detail by powder X-ray diffraction (XRD), scanning electron microscopy (SEM), and transmission electron microscopy (TEM).

Introduction

Titanium dioxide has great potential in pigments, sensors, dielectric ceramics, as a catalyst supporter, and in solar cells as it exhibits outstanding ability for deodorization, air purification, and sterilization by strong photocatalysis.[1–10] Its performance depends to a large extent on its physical and chemical nature, which are related to its crystal structure, grain (crystal) size, morphology, and even surface structure.[11] Therefore, there is considerable interest in the controlled preparation of TiO_2 with a specific nanostructure.[12–24]

Many chemical routes have been developed to synthesize titania nanoparticles, typically gas condensation and wet chemistry.[25–32] In the former, it is not easy to control grain size and crystal shape; in addition, there are some limitations such as low output, complex equipment, and high cost. In contrast, it is much easier to control and modify the growth by adopting appropriate organic ligands in wet chemical processing such as sol–gel and hydrothermal synthesis.

[a] State Key Laboratory of Optoelectronic Materials and Technologies, School of Chemistry and Chemical Engineering, Sun Yat-Sen (Zhongshan) University,
Guangzhou, 510275, P. R. China,
Fax: +86-20-8403-6766
E-mail: ceswmm@sysu.edu.cn
[b] Department of Earth and Planetary Sciences, Johns Hopkins University,
Baltimore, MD 21218, USA
[c] Department of Geology and Geophysics, University of Wisconsin,
Madison, Wisconsin 53706, USA

The sol–gel approach provides a feasible route to prepare nanosized particles by using organic ligands to confine the growth. However, the high-temperature calcination may lead to aggregation into larger particles, phase transformation, and unavoidable evaporation of organic molecules. More attention has been paid to hydrothermal synthesis because of its much milder and friendly reaction conditions in a tightly closed vessel, and it shows advantages over sol–gel processes in most aspects.[30,31]

Multidispersed nanocrystals are generally produced because of the heterogeneous nature of the reaction and Ostwald ripening during hydrothermal aging. Therefore, the use of an organic solvent as a reaction medium[16,32] and of organic surfactants as ligands to confine the growth has raised great interest.[21,22] It has been reported that rutile nanofibers and poorly crystalline, multidispersed anatase nanoparticles can be prepared using alcohols as solvents.[33] In the first part of this manuscript, we will use *n*-butyl alcohol instead of water as a nonaqueous reaction medium and titanium *n*-butoxide (TNB) as a titanium precursor to prepare monodispersed anatase TiO_2 nanocubes.

Besides the use of organic surfactants with long alkyl chains, some smaller organic acids and amines with oxygen and nitrogen as donors have also been employed to modify the growth of titania in aqueous or nonaqueous solvents.[17,34] For example, Sugimoto and co-workers have investigated organic amines for the shape-controlled synthesis of TiO_2 nanoparticles by employing titanium isopropoxide as a titanium source[29] while Jiang and co-workers have investigated carboxylic acids for the size-controlled synthesis of TiO_2 by employing inorganic metatitanic acid as a

titanium source.[35] The use of diols in an autoclave synthesis of nanosized TiO_2 crystals has also been reported in several papers.[36,37] Herein we compare the use of organic diamines, diacids, and diols as additives on the growth of TiO_2 nanocrystals in a sol–hydrothermal approach.

As with the use of organic molecules, inorganic acidic aqueous solutions have been extensively used in the past few decades to precipitate TiO_2 nanocrystals. Besides our previous work, the influence of some small inorganic acids such as HCl on the growth of products has been investigated in detail.[30,38,39] Recently, the growth process of TiO_2 nanocrystals is receiving more and more interests.[40–42] However, to the best of our knowledge there are no reports about the evolution of one-dimensional rutile nanostructures with hydrothermal growth and aging. Such a growth and aging process of pure-phase rutile nanocrystals is investigated here in detail based on our previous work.[30]

Results and Discussion

The Use of Pure Water as Solvent

TNB is very reactive towards nucleophilic reagents and its hydrolysis occurs very easily in water. However, its hydrolysis can be modified and the growth of the resultant TiO_2 controlled by organic alcohols, acids, and even amines. A comparable experiment was performed without adding any additive or co-solvent to investigate the effect of alcohol, acid, and amine on the crystallization of TiO_2. The powder XRD pattern shown in part a of Figure 1 reveals that TiO_2 particles from "pure hydrothermal treatment" of TNB crystallize in phase-pure tetragonal anatase (JCPDS card no. 84-1286) in the space group $I4_1/amd$ (no. 141) with unit cell dimensions a = 0.3782 and c = 0.9502 nm. The TEM image in Figure 1 (b) demonstrates that most of the particles range from 10 to 20 nm in size and are finely dispersed. The crystal sizes calculated from the 101 and 200 diffractions using Scherrer's equation are 15.7 and 12.2 nm, respectively. The ratio of D_{101}/D_{200} is about 1.30, which indicates some anisotropic growth. A few aggregates and much larger particles can be clearly observed, which is probably due to the easy hydrolysis of TNB, precipitation of amorphous titania particles, and heterogeneous reactions. In order to obtain more uniform titania nanocrystals, organic solvents such as *n*-butyl alcohol were used as solvents and/or chelating ligands to inhibit hydrolysis and manipulate the growth of TiO_2.

The Use of Organic Compounds

n-Butyl Alcohol as Solvent

Recently, highly crystalline anatase nanoparticles have been synthesized by the reaction of titanium tetraisopropoxide with common ketones and aldehydes as oxygen-supplying agents under solvothermal conditions.[32] In our present work, highly crystalline and monodispersed anatase nanocrystals are obtained in *n*-butyl alcohol. TNB is dissolved in *n*-butyl alcohol to form a transparent sol. This homogeneous sol can be used in a solvothermal reaction to prepare uniform TiO_2 nanocrystals. During the synthesis, the etherification of *n*-butyl alcohol in the system would occur and slowly generate water, which could play a role as an oxygen donor in the hydrolysis of TNB to form titania.[33]

The powder XRD pattern (Figure 2, a2) indicates the product is phase-pure anatase. The calculated crystallite

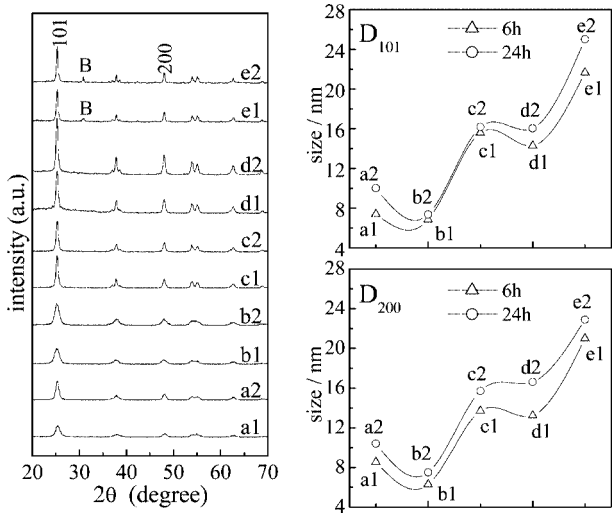

Figure 2. XRD patterns (left panel) of TiO_2 powders derived from several different media at 220 °C after 6.0 h (a1–e1) and 24 h (a2–e2), and a comparison of the corresponding calculated particle sizes by fitting the FWHM of (101) (top-right panel) and (200) (bottom-right panel) peaks: (a) *n*-butyl alcohol, (b) 1,2-propanediol, (c) propanedicarboxylic acid, (d) butanedicarboxylic acid, (e) ethylenediamine. B means Brookite.

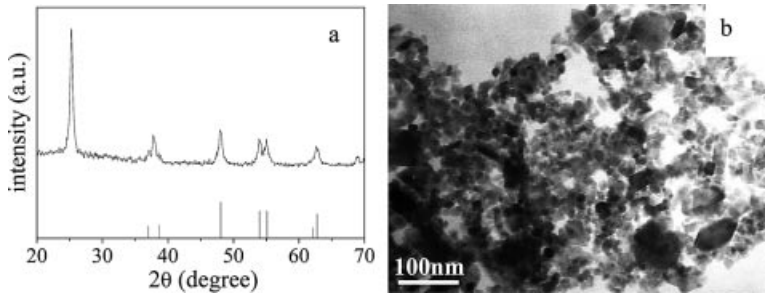

Figure 1. (a) Powder XRD pattern of the nanocrystalline titania product generated in "pure water" at 220 °C for 24 h (top), and pattern with vertical bars (bottom) derived from the JCPDS card (no. 84-1286) of anatase TiO_2. (b) TEM image of the product.

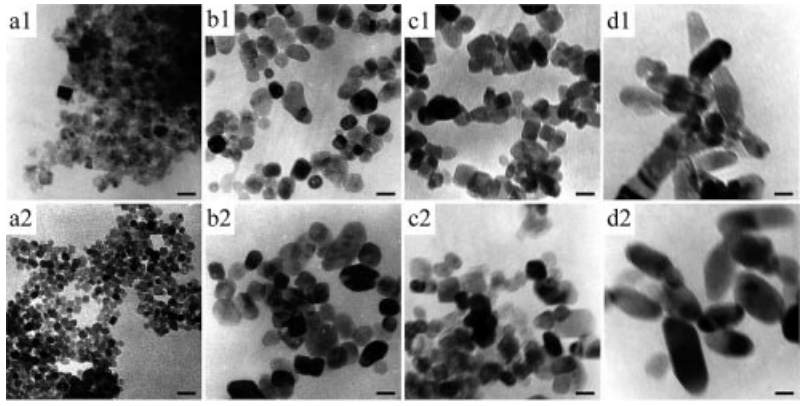

Figure 3. TEM images of nanocrystalline TiO_2 samples obtained under various sol–hydrothermal conditions: (a) *n*-butyl alcohol, (b) propanedicarboxylic acid, (c) butanedicarboxylic acid, (d) ethylenediamine. Scale bar: 20 nm.

sizes are 10.0 (D_{101}) and 10.4 nm (D_{200}), which imply an isotropic growth of TiO_2 nanocrystals. Besides the crystal sizes, the particle sizes of TiO_2, as displayed in Figure 3 (a2), are smaller than those in Figure 1 (b), further confirming that the use of *n*-butyl alcohol can confine the growth of titanium dioxide. Besides acting as an oxygen donor, *n*-butyl alcohol is also the by-product of the hydrolysis of TNB, therefore the use of *n*-butyl alcohol as a solvent would significantly retard the hydrolysis, polycondensation, and eventual crystallization and growth. More significantly, monodispersed nanocubes of highly crystalline anatase crystals are obtained from such a solvothermal growth in *n*-butyl alcohol.

An Organic Diol

In order to compare the effect of a monoalchol and diol on the growth of TiO_2, 1,2-propanediol was used as an additive. A homogeneous sol of the precursor was formed by mixing TNB and 1,2-propanediol with magnetic stirring before performing the reaction. The product was indexed to be anatase, with crystallite sizes of 7.4 (D_{101}) and 7.5 nm (D_{200}; Figure 2, b2), which also indicate an isotropic growth as compared to that obtained with *n*-butyl alcohol. However, 1,2-propanediol inhibits the growth of TiO_2 more, probably due to its stronger chelating ability because of its didentate structure.

Organic Diacids

A carboxyl group could serve as a donor to coordinate titanium atom in aqueous solution,[35] and organic acids can serve as ligands to limit the hydrolysis of TNB. Thus, a homogeneous hydrosol was produced as a hydrothermal reaction precursor for the formation of uniform titania nanoparticles. Herein, propanedicarboxylic acid and butanedicarboxylic acid were chosen as additives in the reaction media to modify the hydrothermal growth of TiO_2. The products were identified from their powder XRD patterns to be anatase (parts c2 and d2 in Figure 2). Highly dispersed nanoparticles, as shown in Figure 3 (see b2 and c2), are clearly obtained. Although organic diacids could be used as ligands to complex titanium atoms and might confine the growth of TiO_2 crystals, in our present work the calculated crystal sizes (D_{101} = 16.2, D_{200} = 15.7 nm and D_{101} = 16.2, D_{200} = 16.6 nm for propanedicarboxylic acid and butanedicarboxylic acid, respectively) are a little larger than those from a "pure hydrothermal reaction", and are much larger than those from alcohols (Figure 2, right panel). Thus, the ability of these diacids to confine the growth is greatly reduced. This can be attributed to the presence of H_3O^+ ions[30,31] and esterification of the acid with *n*-butyl alcohol, which is the by-product of the hydrolysis of TNB. In this way, the chelating ability of the acid is greatly reduced.

A Diamine

The titanium dioxide product from the reaction with the addition of ethylenediamine is anatase with a trace of brookite (Figure 2, e2). The existence of brookite might result from the weakly basic nature of the amine.[43]

The crystal sizes of the product are related to both nucleation and growth: a greater number of nuclei generally result in a smaller crystal size. The isoelectronic point (IEP) of titania is around pH 6. In either basic or acidic medium, the solubility of titania is greater than that in both alcohol and water, which means that the number of nucleation sites in either a basic or acidic medium is less than that in alcohol. Therefore, the sizes of crystals grown in either acidic or basic medium should be larger than those grown in alcohol or water. In addition, it has been well established that both organic amines and acids can catalyze the growth of titania particles.[13,30] The crystal sizes, as shown in Figure 2 (e2), are larger than those from alcohol (parts a2 and b2 in Figure 2).

Figure 3 (d2) reveals that the use of ethylenediamine can significantly promote an anisotropic growth of TiO_2 nanocrystals and, consequently, TiO_2 nanorods are obtained. The anisotropic growth of anatase is attributed to its stronger adsorption of ethylenediamine onto the crystal faces parallel to the *c*-axis than the others.[29] This organic diamine is a strong ligand for some transition metals such as zinc, copper, and nickel, and is widely used in coordination chemistry.[44] However, the capping ability of nitrogen

atoms − the electron donors in amines − with titanium is relatively weaker than the oxygen atoms in carboxyl moieties or hydroxide ions. Therefore, the particle sizes of the final products obtained from the aqueous solution of ethylenediamine are significantly larger than those from the organic media mentioned above (Figure 2).

Reaction Times

In order to further investigate the growth behavior of TiO_2 in various reaction media in the presence of organic alcohol, acid, or amine, the reaction time was shortened to six hours. The powder XRD and TEM images in Figures 2 and 3, respectively, confirm similar growth features to those observed after 24 h, and it can also be observed that the crystal sizes of TiO_2 from the amine medium are the largest and those from the alcohol medium are the smallest. However, some titania particles are not well crystallized after a crystallization time of only 6.0 h, as observed in Figure 3 (a1).

Well-crystallized anatase particles can be observed after only a short time either in butanediacarboxylic acid or in propanedicarboxylic acid. Anatase crystals exhibit very similar growth behavior in these two organic acids. The TEM images and calculated crystal sizes indicate a similar isotropic growth behavior of TiO_2 nanocrystals in the presence of these organic acids, which have similar structures except for the length of their alkyl chain.

The resultant crystal sizes are dependent on a cooperative effect of hydrolysis, nucleation, growth, and aging. Beside the growth, the other fundamental significance for studying the size and shape control of the nanocrystals lies in the understanding of their nucleation. Facile hydrolysis, such as in "pure water", might yield larger amount of nuclei and reduce crystal sizes, especially without aging, although it could also shorten the time to reach the nucleation and growth step, which might increase the crystal sizes. Therefore, the role of the nucleation and its effect on the crystal sizes is quite complicated and generally poorly understood due to a lack of reliable experimental data.[45] Here, for example, the growth of anatase crystals in alcohol, particularly in the diol, is obviously inhibited, whereas in amine it is considerably accelerated (Figure 2, right panel). In summary, the ability to retard the growth of anatase follows the trend 1,2-propanediol > *n*-butyl alcohol > water > butane(or propane)dicarboxylic acid > ethylenediamine, with the donor sequence OH, COO^-, NH_2. Based on these experimental results, we are convinced that the growth step generally plays a crucial role during the hydrothermal reaction.[17] Therefore, in order to obtain optimal nanostructured materials, it is quite important to adopt appropriate organic molecule to modify the growth behavior.[45,46]

The Use of Inorganic Acids: A Typical Growth and Aging of Rutile in Hydrochloric Acid

In our previous work we investigated the effects of inorganic acids on the growth of TiO_2 and found that pure-phase anatase, a mixture of anatase and rutile, and pure-phase rutile were obtained in acetic acid, nitric acid, and hydrochloric acid, respectively.[30] It has also been reported that pure rutile can be grown in nitric acid.[47] However, upon changing the TNB and nitric acid concentrations from those in the literature,[30,47] no rutile phase appeared, and phase-pure anatase was formed instead. This suggests that the growth of TiO_2 in nitric acid is very complicated. The anatase products formed as nanograins and rutile as nanorods (Figure 4, right panel, parts b and c).

We have previously reported the synthesis of rutile nanocrystals at temperatures above 200 °C by using TNB as a starting material in sol–hydrothermal reactions. A low-temperature preparation of rutile nanorods was also achieved at around 100 °C by using either titanium tetrachloride or trichloride as titanium source.[33,40] However, titanium chlorides release large amounts of heat, which prevents the homogeneous precipitation of TiO_2 particles because of the vigorously exothermic reaction, when titanium chloride is dissolved in water.[15,30]

According to the above experimental results with inorganic media (Figure 4), it can be concluded that phase-pure rutile nanorods can be formed in HCl. Therefore, HCl solution was selected as a representative inorganic medium to examine the growth of rutile at a much lower temperature. We used a modified sol–hydrothermal growth to prepare

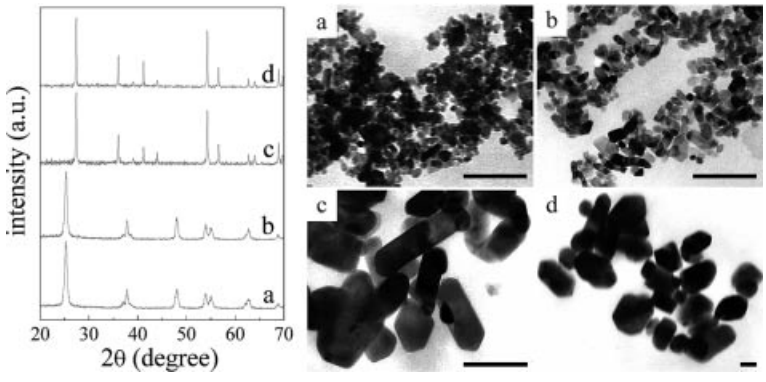

Figure 4. XRD patterns and TEM images of titania samples generated from various solutions at 220 °C: (a) HOAc, (b) HNO_3, and (c) HCl for 24 h; (d) HCl for 7 d. Scale bar: 100 nm.

rutile nanoneedles with a much higher aspect ratio at 100 and 140 °C, respectively. As indicated in Figure 5 (a1), rutile was obtained as the exclusive product at 100 °C after only two hours. The nanoparticles of rutile prepared at this point are highly aggregated into nanospheres consisting of very thin nanorods (Figure 6, a1 and inset). Their radial assembly in a good geometrical match to create the spherical nanostructure could significantly reduce the total free energy. These spherical structures are present for about 10 h at 100 °C and are then destroyed by further hydrothermal reaction (Figure 6, a4). The calculated crystalline sizes of rutile prepared at 100 °C after two hours are about 2.1 and 5.5 nm for the 110 and 101 diffractions, respectively. With an increase of reaction time, the crystal sizes assigned to D_{110} tend to increase progressively. However, the crystal sizes calculated from the 101 diffraction tend to increase only up to 10 h and decrease a little thereafter (Figure 5, middle).

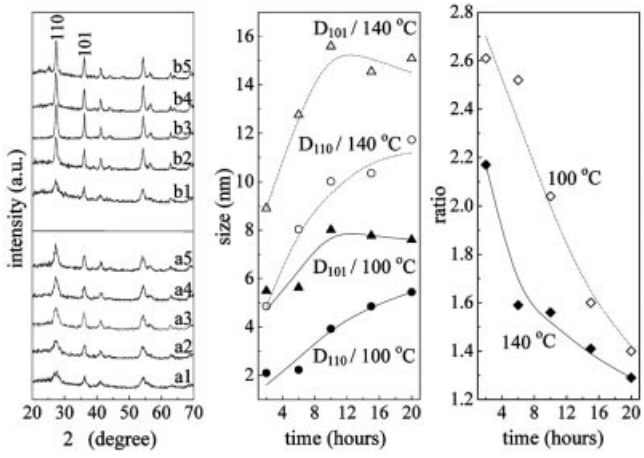

Figure 5. XRD patterns (left panel) of the products formed with HCl at 100 °C (a1–a5) and 140 °C (b1–b5) after 2.0 h (a1, b1), 6.0 h (a2, b2), 10 h (a3, b3), 15 h (a4, b4), and 20 h (a5, b5). Crystallite sizes (middle panel) calculated by fitting the FWHM of the (110) and (101) peaks. D_{101}/D_{110} ratios (right panel).

Phase-pure rutile can also be obtained at 140 °C (Figure 5, b1) and a similar hydrothermal growth behavior to that at 100 °C is observed (Figure 5, middle). These rutile particles synthesized at 140 °C also self-aggregate into microspheres up to 10 h (Figure 6, b1–b3). However, the aggregated microspheres self-disperse after a longer hydrothermal aging such as for 15 h (Figure 6, b4). This might be due to a much higher activation energy for self-aggregation for the formation of larger nanorods. The typical product obtained at 140 °C after 10 h consists of well-defined nanoneedles, as clearly illustrated in Figure 7 (a), in which the sample for TEM observation has been highly and strongly ultrasonically dispersed. The anisotropic growth of rutile nanoneedles into self-assembled sub-microspheres can clearly be observed in the low-magnification TEM image (Figure 7, b). The lattice spacing of 0.32 nm perpendicular to the longitudinal direction in the high-magnification TEM image implies a <001> growth direction (Figure 7, c). The favorable growth along the *c*-axis in the early stages is due to the internal structure, as we described previously.[30] The growth velocity at the initial stage either in the radial or longitudinal direction is much faster than that at 100 °C due to kinetic factors. This type of quick growth feature during the initial stage has been well documented by Peng for semiconductors.[45] With further aging after 10 h, the radial growth tends to be slower and the longitudinal growth also tends to be retarded. The maximum value

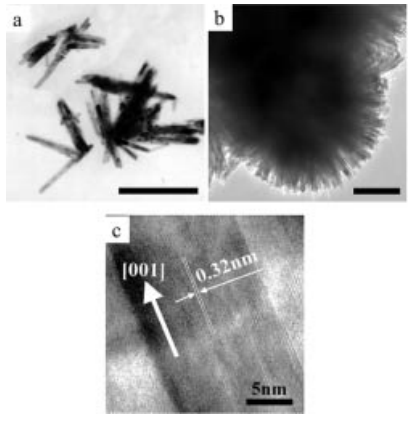

Figure 7. TEM images of ultrasonically dispersed rutile nanoneedles (a), a self-assembled sphere (b), and a high-resolution TEM image of a specific nanoneedle (c). Scale bar: 200 nm.

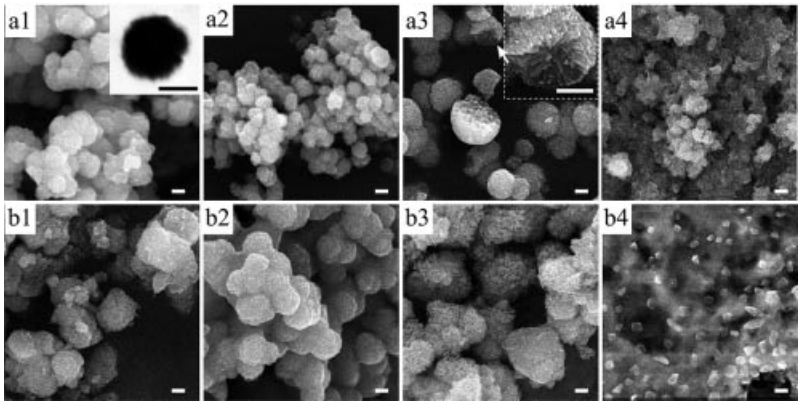

Figure 6. Electron microscopy images of the products obtained with HCl at 100 °C (a1–a4) and 140 °C (b1–b4) after 2.0 h (a1, b1), 6.0 h (a2, b2), 10 h (a3, b3), and 15 h (a4, b4). The inset in a3 is the magnified sphere indicated by the white arrow. Scale bar: 200 nm.

of D_{101} at 10 h and the slow decrease of D_{101} after 10 h (Figure 5, middle) reveals an obvious 1D/2D ripening during hydrothermal aging, as described previously for CdSe nanorods.[45]

The ratio of D_{101}/D_{110} indicates that the aspect ratio drops noticeably with hydrothermal reactions longer than two hours in our present work. We did not observe the 1D and 3D growth stage described previously by Peng for the growth of CdSe nanocrystals[45] when our reaction is shorter than two hours (Figure 5, right panel). However, both the short and long axes increase when the reaction time is shorter than 10 h at either 100 °C or 140 °C (Figure 5, middle). Thus, the reaction at times shorter than 10 h can be referred to as a three-dimensional growth stage. After 10 h, the short axis keeps growing while the long axis becomes shorter. There is therefore a noticeable net growth and net dissolution along the short and long axes, respectively, along with a 1D/2D ripening. This produces nanorods with smaller aspect ratios, and granular particles are produced if allowed enough reaction time. A significant experimental result in our present work is that the aspect ratio at 100 °C is greater than that at 140 °C, as shown in Figure 5 (right). This means that the higher reaction temperature accelerates the 1D/2D ripening, especially for longer reaction times. For example, many more and larger granular crystals are noticeable at 220 °C after one day, and even more so after seven days (Figure 4, c, d, right).

Conclusions

A variety of sol–hydro(solvo)thermal syntheses of anatase and rutile nanocrystals have been comparatively described that use small inorganic and organic compounds as additives at various reaction temperatures for different aging times. Instead of water, alcohol as a solvent in the sol–hydrothermal synthesis can result in a confined growth of well-crystalline and uniform anatase nanocubes. Except for HCl medium, phase-pure anatase can be formed in an organic alcohol, an organic diamine, an organic diacid, and acetic and nitric acids. The use of a diamine promotes the anisotropic growth of anatase nanocrystals, while the use of a diacid cannot do this efficiently because of its stronger capping ability. Rutile nanospheres self-assembled from rutile nanorods are obtained through a facile sol–hydrothermal growth route in HCl medium. More significantly, a 3D growth and 1D/2D ripening mechanism of rutile nanocrystals are revealed. It is proposed that prolonging the reaction time and increasing the reaction temperature will lead to the formation of larger rutile crystals but will reduce the aspect ratios of one-dimensional rutile nanocrystals.

Experimental Section

Preparation: Titanium salts such as titanium chloride ($TiCl_3$ or $TiCl_4$),[40,42] titanium sulfate $Ti(SO_4)_2$,[48,49] and titanium alkoxide $[Ti(OR)_4]$[30,41] in solution are often used as titanium sources to synthesize TiO_2 nanoparticles. The hydrolysis of $Ti(OR)_4$ is relatively mild as compared with inorganic salts and is easy to control. Therefore, tetrabutyl titanate was employed here as the titanium source. In the present work, besides H_2O and *n*-butyl alcohol as "pure solvents", the others were used as aqueous 2.0 M solutions of acetic acid, nitric acid, hydrochloric acid, 1,3-propanedicarboxylic acid, 1,4-butanedicarboxylic acid, 1,2-propanediol, and ethylenediamine. Titanium *n*-butoxide $[Ti(OC_4H_9)_4$, TNB] was added dropwise to one of the pure organic solvents or one of the concentrated inorganic acids/amine under magnetic stirring to form a clear sol. Then, distilled water was added dropwise to the sol while stirring to prepare a reagent with a fixed concentration of diol, acid, amine, and titanium (2.0 M). Subsequently, the homogeneous hydrosol was transferred into a Teflon-lined stainless-steel vessel, which was tightly closed instantly for sol–hydrothermal reaction under an autogenous pressure at 220 °C for one day, unless otherwise mentioned. The vessel was then taken out from the oven and cooled to ambient temperature. The white product was filtered, washed with distilled water, and dried in a desiccator at ambient temperature.

Characterization: Products were characterized by powder X-ray diffraction using Cu-K_α radiation (λ = 0.15045 nm) and a graphite monochromator on a RIGAKUD/MAX 2200 VPC diffractometer operating at 40 kV and 30 mA. Crystallite sizes of TiO_2 particles were calculated using Scherrer's equation from the FWHM (full-width at half-maximum) of the anatase (101 and 200) and rutile (110 and 101) diffractions, respectively. Electron microscopy observations were carried out with a JSM-6330F Field Emission scanning electron microscope at 15 kV or JEM-100CX and JEM-2010 transmission electron microscopes at 100 kV and 200 kV, respectively. The samples for TEM examination were prepared by depositing an ultrasonically dispersed suspension of TiO_2 powder from a water/alcohol mixture onto a carbon-coated copper grid.

Acknowledgments

This work was supported financially by the Natural Science Foundation of China, the NSF of Guangdong Province, and the government of Guangzhou City.

[1] B. O'Regan, B. M. Grätzel, *Nature* **1991**, *353*, 737–740.
[2] M. K. Nazeeruddin, A. Kay, L. Rodicio, R. Humphry-Baker, E. Müler, P. Liska, N. Vlachopoulos, M. Grätzel, *J. Am. Chem. Soc.* **1993**, *115*, 6382–6390.
[3] J. Karch, R. Birriger, H. Gleiter, *Nature* **1987**, *330*, 556–558.
[4] R. Wang, K. Hashimoto, A. Fujishima, *Nature* **1997**, *388*, 431–432.
[5] S.-Q. Liu, A.-C. Chen, *Langmuir* **2005**, *21*, 8409–8413.
[6] M. R. Hoffmann, S. T. Martin, W. Choi, D. W. Bahnemann, *Chem. Rev.* **1995**, *95*, 69–96.
[7] L.-X. Cao, Z. Gao, S. L. Suib, T. N. Obee, S. O. Hay, J. D. Freihaut, *J. Catal.* **2000**, *196*, 253–261.
[8] J. Shang, M. Chai, Y.-F. Zhu, *J. Solid State Chem.* **2003**, *174*, 104–110.
[9] U. Diebold, *Surf. Sci. Rep.* **2003**, *48*, 53–229.
[10] C.-F. Lao, Y.-T. Chuai, L. Su, X. Liu, L. Huang, H.-M. Cheng, D.-C. Zou, *Sol. Energ. Mater. Sol. C* **2005**, *85*, 457–465.
[11] R. W. Siegal, S. Ramasamy, H. Hahn, Z.-Q. Li, T. Lu, R. Gronsky, *J. Mater. Res.* **1988**, *3*, 1367.
[12] Z.-R. Tian, J. A. Voigt, J. Liu, B. McKenzie, H.-F. Xu, *J. Am. Chem. Soc.* **2003**, *125*, 12384–12385.
[13] A. Chemseddine, T. Moritz, *Eur. J. Inorg. Chem.* **1999**, *2*, 235–245.
[14] Y. Li, T. J. White, S. H. Lim, *J. Solid State Chem.* **2004**, *177*, 1372.

[15] W. Wang, B.-H. Gu, L.-Y. Liang, W. A. Hamilton, D. J. Wesolowski, *J. Phys. Chem. B* **2004**, *108*, 14789–14792.
[16] X.-C. Jiang, T. Herricks, Y.-N. Xia, *Adv. Mater.* **2003**, *15*, 1205–1209.
[17] P. D. Cozzoli, A. Kornowski, H. Weller, *J. Am. Chem. Soc.* **2003**, *125*, 14539–14548.
[18] J. Tang, F. Redl, Y.-M. Zhu, T. Siegrist, L. E. Brus, M. L. Steigerwald, *Nano Lett.* **2005**, *5*, 543–548.
[19] J. Polleux, N. Pinna, M. Antonietti, M. Niederberger, *Adv. Mater.* **2004**, *16*, 436–439.
[20] B.-M. Wen, C.-Y. Liu, Y. Liu, *Chem. Lett.* **2005**, *34*, 396–397.
[21] B.-M. Wen, C.-Y. Liu, Y. Liu, *New J. Chem.* **2005**, *29*, 969–971.
[22] S.-W. Yang, L. Gao, *Chem. Lett.* **2005**, *34*, 964–965.
[23] S.-W. Yang, L. Gao, *Chem. Lett.* **2005**, *34*, 972–973.
[24] J. M. Macák, H. Tsuchiya, P. Schmuki, *Angew. Chem. Int. Ed.* **2005**, *44*, 2100–2102.
[25] V. G. Besserguenev, R. J. F. Pereira, M. C. Mateus, I. V. Khmelinskii, E. Burkel, R. C. Nicula, *Int. J. Photoenergy* **2003**, *5*, 99–105.
[26] S. Seifried, M. Winterer, H. Hahn, *Scr. Mater.* **2001**, *44*, 2165–2168.
[27] E. Beyers, P. Cool, E. F. Vansant, *J. Phys. Chem. B* **2005**, *109*, 10081–10086.
[28] A. K. John, G. D. Surender, *J. Mater. Sci.* **2005**, *40*, 2999–3001.
[29] T. Sugimoto, X.-P. Zhou, A. Muramatsu, *J. Colloid Interface Sci.* **2003**, *259*, 53–61.
[30] M.-M. Wu, G. Lin, D.-H. Chen, G.-G. Wang, D. He, S.-H. Feng, R.-R. Xu, *Chem. Mater.* **2002**, *14*, 1974–1980.
[31] H.-M. Cheng, J.-M. Ma, Z.-G. Zhao, L.-M. Qi, *Chem. Mater.* **1995**, *7*, 663–671.
[32] G. Garnweitner, M. Antonietti, M. Niederberger, *Chem. Commun.* **2005**, *3*, 397–399.
[33] C. Wang, Z.-X. Deng, G.-H. Zhang, S.-H. Fan, Y.-D. Li, *Powder Technol.* **2002**, *125*, 39–44.
[34] M. Ivanda, S. Music, S. Popovic, M. Gotic, *J. Mol. Struct.* **1999**, *481*, 645–649.
[35] B.-P. Jiang, H.-B. Yin, T.-S. Jiang, J. Yan, Z. Fan, C.-S. Li, J. Wu, Y. Wada, *Mater. Chem. Phys.* **2005**, *92*, 595–599.
[36] S. Iwamoto, K. Saito, M. Inoue, *Nano Lett.* **2001**, *1*, 417–421.
[37] W. Payakgula, O. Mekasuwandumrongb, V. Pavarajarna, P. Praserthdama, *Ceram. Int.* **2005**, *31*, 391–397.
[38] C.-C. Wang, J.-Y. Ying, *Chem. Mater.* **1999**, *11*, 3113–3120.
[39] S. T. Aruna, S. Tirosh, A. Zaban, *J. Mater. Chem.* **2000**, *10*, 2388–2391.
[40] X. Bokhimi, A. Morales, F. Pedraza, *J. Solid State Chem.* **2002**, *169*, 176–181.
[41] S. Hyunho, S. J. Hyun, S. H. Kug, L. Jung-Kun, *J. Solid State Chem.* **2005**, *178*, 15–21.
[42] G.-S. Li, L.-P. Li, J. Boerio-Goates, B. F. Woodfield, *J. Am. Chem. Soc.* **2005**, *127*, 8659–8666.
[43] J.-G. Li, C.-C. Tang, D. Li, H. Haneda, T. Ishigaki, *J. Am. Ceram. Soc.* **2004**, *87*, 1358–1361.
[44] E. G. S. Michael, A. C. David, M. Philip, *Chem. Commun.* **2000**, *13*, 1167–1168.
[45] Z.-A. Peng, X.-G. Peng, *J. Am. Chem. Soc.* **2001**, *123*, 1389–1395.
[46] X. Wang, J. Zhuang, Q. Peng, Y.-D. Li, *Nature* **2005**, *437*, 121–124.
[47] Y.-T. Qian, Q.-W. Chen, Z.-Y. Chen, C.-G. Fan, G.-E. Zhou, *J. Mater. Chem.* **1993**, *3*, 203–205.
[48] H. K. Park, Y. T. Moon, D. K. Kim, C. H. Kim, *J. Am. Ceram. Soc.* **1996**, *79*, 2727–2732.
[49] M. Iwasaki, M. Hara, S. Ito, *J. Mater. Sci. Lett.* **1998**, *17*, 1769–1771.

Received: September 26, 2005
Published Online: March 31, 2006

